JACS
JOURNAL OF THE AMERICAN CHEMICAL SOCIETY
Article
pubs.acs.org/JACS

Stepwise Construction of an Iron-Substituted Rigid-Rod Molecular Wire: Targeting a Tetraferra−Tetracosa−Decayne

Franziska Lissel,[†] Thomas Fox,[†] Olivier Blacque,[†] Walther Polit,[#] Rainer F. Winter,[#] Koushik Venkatesan,[†] and Heinz Berke*[,†]

[†]Institute of Inorganic Chemistry, University of Zürich, Winterthurerstrasse 190, CH-8057 Zürich, Switzerland
[#]Faculty of Chemistry, University of Konstanz, Universitätsstrasse 10, D-78457 Konstanz, Germany

Supporting Information

ABSTRACT: *trans*-Fe(depe)$_2$I$_2$ (depe =1,2-bis(diethylphosphino)ethane) was employed to stepwise incorporate Fe(II) centers into a rigid-rod butadiyne based 5,10,15,20-tetraferratetracosa-1,3,6,8,11,13,16,18,21,23-decayne. The iterative synthesis first connects two Fe(II) centers via a central butadiynediyl ligand to provide I-Fe(depe)$_2$-C$_4$-Fe(depe)$_2$-I (**2**), then extends the system by substituting the terminal halides of **2** to yield Me$_3$SiC$_4$-Fe(depe)$_2$-C$_4$-Fe(depe)$_2$-C$_4$SiMe$_3$ (**3**). Further modification of the termini gives the deprotected and stannylated compounds RC$_4$-Fe(depe)$_2$-C$_4$-Fe(depe)$_2$-C$_4$R (**4** and **5**; R = H, Sn(CH$_3$)$_3$, respectively). Transmetalation with two more mononuclear units furnishes the homometallic tetranuclear compound I-Fe(depe)$_2$-C$_4$-Fe(depe)$_2$-C$_4$-Fe(depe)$_2$-C$_4$-Fe(depe)$_2$-I (**6**), to which two more butadiynyl units were attached to give Me$_3$SiC$_4$-Fe(depe)$_2$-C$_4$-Fe(depe)$_2$-C$_4$-Fe(depe)$_2$-C$_4$-Fe(depe)$_2$-C$_4$SiMe$_3$ (**7**). All compounds were characterized by NMR, IR, and Raman spectroscopies and by elemental analyses. X-ray diffraction studies were carried out on the dinuclear complexes revealing highly symmetrical rigid-rod structures. Cyclic voltammetric studies showed that compounds **2**−**7** undergo reversible and well-defined oxidations with high K_c values indicating thermodynamically stable mixed valence species. While the number of the oxidation waves of compounds **2**, **6**, and **7** are equivalent to the number of metal centers, the dinuclear complexes **3**, **4**, and **5** exhibit three reversible oxidation waves, one at significantly more positive potential. Two redox waves were attributed to the oxidation of the metal centers, while the remaining one is due to the oxidation of the butadiynediyl ligand. The electronic properties of complexes **2**, **3**, and **7** were investigated by spectroelectrochemical measurements.

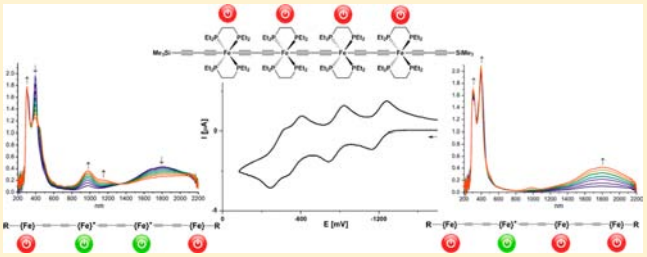

INTRODUCTION

Molecular-scale electronics seeks to assemble appropriate molecular components for exerting specific functions in molecular electronic devices.[1,2] One of the basic functions required for many types of electronic devices on the molecular level is based on the design of π-conjugated rigid-rod molecules, so-called "molecular wires", that are able to transport electric charge over distances of several nanometres.[3] The electron transport through single molecules and ultimately the relationship between molecular structure and electric or electronic properties is as yet not fully understood.[4] Nevertheless, conjugated organic moieties, especially those consisting of sp-hybridized carbon atoms, constitute materials that accomplish high electron transfer rates, since they provide well-defined, fully conjugated, rigid-rod structures with strongly delocalized frontier orbitals.[5] Tunnelling-based charge transfer rates of purely organic "conducting" systems are known to decay exponentially with the distance until, at certain length, the tunnelling turns into a multistep hopping having a nonexponential distance dependence.[6,7] As has been exemplified by terpyridine-based frameworks, the so-called "relay approach", that is the insertion of metal centers into rigid-rod architectures, promotes transport based on electron hopping by providing defined donor−acceptor sites, thus enhancing the overall conductivity.[8]

Transition metal polycarbyl complexes of the type L$_m$M-(C$_n$)-ML$_m$ have received considerable attention in recent years due to their potential as molecular wires.[9−14] Electronic delocalization over the length of the unsaturated carbon bridge could be probed by using spectroelectrochemical methods.[15,16] Investigations of this kind were mainly focused on molecules of the type (Cp*)(PP)M-C$_n$-M(PP)(Cp*) (Cp*= η^5-C$_5$Me$_5$, P = monodentate phosphine ligand or PP = bidentate phosphine ligand, C$_n$ = organic bridging ligand),[11,17] which might be called dinuclear stopper-type as they do not possess end groups that allow their connection to electrodes or further extension of the conjugated system. Intrinsically open dinuclear systems of the type X-(PP)M-C$_4$-M(PP)-X (X = halide) are known, but are quite rare.[18−21] The construction of terminally open, metal-containing analogues of higher nuclearities as genuine representatives of the relay approach is synthetically challenging and was up to date only reported for three C$_2$C$_6$H$_4$C$_2$ bridged trinuclear ruthe-

Received: January 4, 2013
Published: February 13, 2013

   dx.doi.org/10.1021/ja400078c | J. Am. Chem. Soc. 2013, 135, 4051−4060

nium[22−24] and iron[25] complexes, a mixed ditungsten diiron tetranuclear complex where a central ditungsten ethynylbis(carbyne) fragment was capped with terminal butadiynyl iron moieties,[26] as well as a series of C_8 bridged platinum complexes.[21]

It was demonstrated for dinuclear stopper type molecules that the chemical reversibility of the redox process is highest for C_4 bridged complexes and decreases rapidly with increasing chain lengths or when other forms of sp/sp^2 type bridges are employed.[27] Consequently, the electronically versatile butadiynediyl fragment[28,29] is an ideal linker for the construction of relay-type conducting molecular entities. Also, among the stopper-type molecules, Lapinte and co-workers showed that butadiynediyl bridged diiron complexes have outstanding electrochemical properties,[30,31] especially with regard to the high stabilization of the various oxidized forms[32] and the high metal character of the delocalized HOMOs in all accessible oxidation states.[33]

In this context we targeted the stepwise incorporation of four Fe(II) centers into a pentakis(butadiynediyl)-based framework to obtain a linear homometallic tetranuclear species. Such architecture is, to the best of our knowledge, unprecedented. Electron-donating bidentate diphosphine ligands occupying the equatorial positions were employed to ensure *trans* configuration of the rigid-rod butadiynediyl units and favorable redox properties. As the chosen iron fragments possess potentially open terminal binding sites, smaller dinuclear units could be used as building blocks and elaborated into larger rigid-rod entities containing up to four metal atoms and five C_4 ligands.

SYNTHESIS AND CHARACTERIZATION OF THE DI- AND TETRANUCLEAR COMPLEXES

Synthetic access to dinuclear iron complexes of the general type (Cp*)(PP)Fe-C_n-Fe(PP)(Cp*) can generally be accomplished via the reaction of a mononuclear fragment of the type (Cp*)(PP)FeCl with silylated alkynes in the presence of MeOH and a fluoride source yielding either directly the targeted dinuclear complex[27] or a mononuclear vinylidene complex that can be subjected to oxidative homocoupling.[34,35] Attempts to employ these conditions to prepare a butadiynediyl-bridged dinuclear iron complex with terminal chloro substituents of the type $Cl(PP)_2Fe$-C_4-$Fe(PP)_2Cl$ turned out to be unsuccessful, yielding an interesting non-rigid-rod trinuclear complex instead.[36] Remarkably, only a few examples of dinuclear complexes of the type $X(PP)_2Fe$-C_n-$Fe(PP)_2X$ (X = halide, CH_3) with modifiable end groups are described in the literature,[25,37,38] but as yet they are bridged by bis(ethynyl)arylene spacers and their synthetic access is based on complex and not generally applicable routes.[19,20,25]

One should also note that in complexes of the type *trans*-$Fe(PP)_2Cl_2$ (PP = 1,2-bis(dimethylphosphino)ethane, 1,2-bis(diethylphosphino)ethane, 1,2-bis(diisopropylphosphino)-ethane) the bidentate phosphine ligands can reversibly dissociate.[39] While this characteristic property allows substitution reactions on the metal center,[40,41] it simultaneously limits the synthetic options for assembling oligonuclear rigid-rod moieties with two bridging ligands in *trans* position[36] as targeted for this work. Although the lability of a bidentate phosphine ligand increases with the sterical demand,[39] we still chose the depe (depe =1,2-bis(diethylphosphino)ethane) ligand over the less bulky methyl-substituted dmpe (dmpe =1,2-bis-(dimethylphosphino)ethane) to maintain a reasonable solubility of the targeted di- and tetranuclear compounds. Instead of the mononuclear dichloro compound, the corresponding diiodo complex *trans*-$Fe(depe)_2I_2$ was chosen as starting material, since the iodides are more reactive and furthermore known to dissociate readily.[42] Also, the lower solubility of the diiodo complex was perceived to be advantageous for the purification of the targeted compounds as it allows a facile separation of the mononuclear precursor. On the basis of earlier work from our group[26,43] we aimed at utilizing transmetalation reactions for the stepwise construction of a tetrairon chain.

As shown in Scheme 1, transmetalating two units of the mononuclear precursor *trans*-$Fe(depe)_2I_2$[44] (**1**) with Me_3Sn—C≡C—C≡C—$SnMe_3$[45] in refluxing tetrahydrofuran gave the butadiyne-bridged dinuclear complex **2** as a burgundy red solid of low solubility in good yield (88%). The $^{31}P\{^1H\}$ NMR of **2** showed a singlet at 69.8 ppm for the eight equivalent P atoms, which is shifted slightly downfield compared to the mononuclear precursor (δ = 65.9 ppm). The shift can be attributed to the introduction of the carbon-rich C_4 bridging ligand, which, in a resonance form best described as a butadiynediyl, reduces the electron density at the metal center, thus leading to an increased σ-donation of the equatorial ligands toward the iron. The $^{13}C\{^1H\}$ NMR spectrum of **2** did not exhibit signals relating to sp-hybridized carbon atoms. As indicated by NMR studies at 193 K, this is not caused by a fluxional behavior as for instance found in the case of $[CpFe(dppe)]_2(\mu\text{-}C_4)$[35] but originates from the low solubility of compound **2**. A second transmetalation process to substitute the terminal iodides in **2** was not successful even in the presence of catalytic amounts of Cu(I).[46]

Related to the reactions of (Cp*)(PP)FeCl and *trans*-$Fe(PP)_2Cl_2$ cores with lithium-acetylide[47] and sodium-acetylide[37,38] reagents, the targeted elongation was finally achieved by substitution of the terminal iodo ligands with a freshly prepared Li—C≡C—C≡C—$SiMe_3$/LiBr[48] reagent in toluene. Compared to the diiodo precursor **2**, the yellow compound **3** with two terminal C_4TMS (TMS = trimethylsilyl, $SiMe_3$) ligands was found to be highly soluble in nonpolar organic solvents, even in pentane. The increased solubility allowed full characterization by ^1H, $^{13}C\{^1H\}$, $^{31}P\{^1H\}$, and $^{29}Si\{^1H\}$ NMR spectroscopies. The resonances for the $SiMe_3$ groups were observed at 0.17 ppm in the ^1H NMR, at −21.8 ppm in the $^{29}Si\{^1H\}$ NMR, and at 1.39 ppm in the $^{13}C\{^1H\}$ NMR spectra. Besides the expected signals for the primary and secondary carbon atoms of the phosphine ligands and the $SiMe_3$ groups, the $^{13}C\{^1H\}$ NMR spectrum showed six signals of sp-hybridized carbon atoms. This is consistent with the centrosymmetric structure of **3** with one central butadiynediyl and two terminal butadiynyl ligands. Each signal corresponds to two chemically and magnetically equivalent carbon atoms. The signals of the carbon atoms in α-position to the iron centers split into multiplets due to the coupling with the four equatorial P atoms. The $^{31}P\{^1H\}$ NMR spectrum exhibited a singlet at 76.3 ppm, which is markedly shifted downfield compared to **2** due to the influence of two additional butadiynyl units.

The TMS groups were removed under mild conditions employing TBAF in THF (containing 5% H_2O) at room temperature. The resulting C_4H derivative **4** was characterized by ^1H, $^{13}C\{^1H\}$, and $^{31}P\{^1H\}$ NMR spectroscopies. It could be stannylated by using NEt_2SnMe_3[49] in refluxing THF to give the trimethyltin capped species **5**. Both complexes were obtained in reasonably high yields (76% and 89%, respectively).

As for compounds **2** and **3**, no column chromatography was needed to obtain the compounds in an analytically pure state. The deprotection and subsequent stannylation of the terminal

dx.doi.org/10.1021/ja400078c | J. Am. Chem. Soc. 2013, 135, 4051−4060

Scheme 1. Stepwise Synthesis of the Tetraferra−Tetracosa−Decayne Complex 7

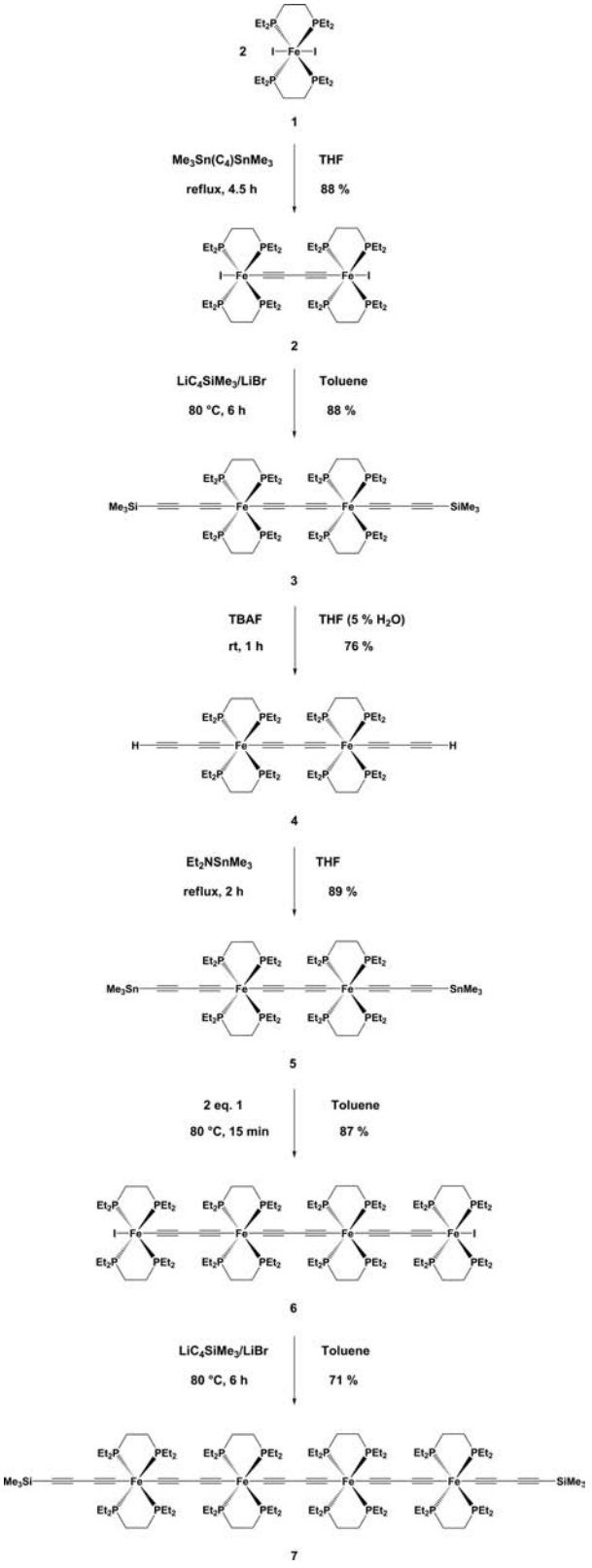

butadiynyl functions has only minor influence on the physical properties.

Similar to the $SiMe_3$ protected **3**, compounds **4** and **5** were yellow solids and highly soluble compared to the diiodo precursor **2**, although **4** was not soluble in pentane. The $^{31}P\{^1H\}$ NMR spectra of both the deprotected and the stannylated diiron complexes displayed singlets at 76.2 or 76.1 ppm, respectively. The $^{13}C\{^1H\}$ NMR spectra showed six signals related to a total of 12 sp-hybridized carbon atoms confirming the centrosymmetry of these rigid-rod molecules. The quintets expected for the carbon atoms in α-position to the iron centers are clearly distinguishable in the spectra of **4**, whereas in the $^{13}C\{^1H\}$ NMR spectrum of the $SnMe_3$-substituted complex **5** only multiplets could be observed for the corresponding signals. The acetylenic proton of **4** was observed as a singlet at 1.26 ppm in the ^1H NMR spectrum in C_6D_6, whereas it coincides with the signals of the methyl groups in THF-d_8. The $SnMe_3$ group of **5** gave rise to a singlet at 0.06 ppm in the ^1H NMR spectrum, at −36.3 ppm in the $^{119}Sn\{^1H\}$ and at −7.47 ppm in the $^{13}C\{^1H\}$ NMR spectra. Both the ^1H and the $^{13}C\{^1H\}$ signals show tin satellites as expected for the $SnMe_3$ functional group. Additional two-dimensional NMR spectra of complexes **2**, **3**, and **4** are displayed in the Supporting Information (see Figures S1−S7).

Transmetalation of **5** with two more mononuclear *trans*-$Fe(depe)_2I_2$ units in toluene (see Scheme 1) resulted in the pale red tetranuclear compound **6**, where four Fe(II) centers are bridged by three butadiynediyl units. The short reaction time of 15 min at 80 °C demonstrated an enhanced reactivity of the terminal C_4SnMe_3 moiety of **5** in comparison with the $Me_3Sn—C{\equiv}C—C{\equiv}C—SnMe_3$ reagent used for the first transmetalation. Similar to the dinuclear diiodo complex **2**, the tetranuclear diiodo complex **6** is poorly soluble, thus limiting the possibilities to characterize this complex by NMR spectroscopy. Two singlets with equivalent integrals appeared in the $^{31}P\{^1H\}$ NMR spectrum, one at 68.3 ppm, in good agreement with the chemical shift of the dinuclear diiodo complex **2** (68.3 ppm), and the other resonance at 77.6 ppm, shifted slightly downfield in comparison with the signals of the three dinuclear C_4R-disubstituted compounds (76.3, 76.2, 76.1 ppm for R = $SiMe_3$, H, $SnMe_3$, respectively).

Substitution of the iodo ligands of **6** with $Li—C{\equiv}C—C{\equiv}C—SiMe_3$/LiBr gave the targeted compound **7**, which was isolated as a dark yellow solid. In the $^{31}P\{^1H\}$ NMR spectrum the signal of the outer $Fe(depe)_2$ centers was found to be shifted downfield to 77.5 ppm, as it is also seen in the other cases of replacement of the iodo ligands with butadiynyl units. Similarly, the $^{31}P\{^1H\}$ NMR signal of the inner $Fe(depe)_2$ entities showed a small shift to 79.3 ppm compared to 77.6 ppm in **6**. Complex **7** contains a centrosymmetric chain of 20 sp-hybridized carbon atoms. As expected, the $^{13}C\{^1H\}$ NMR spectrum exhibits 10 signals for all 20 carbon atoms. Four of these signals correspond to carbon atoms that are directly bonded to the iron centers and are split into multiplets due to the coupling with the P atoms of the depe ligands, while the remaining six signals are singlets.

The $SiMe_3$ functional group was observed as a singlet at 0.18 ppm in the ^1H NMR, at −22.1 ppm in the $^{29}Si\{^1H\}$ NMR and at 1.43 ppm in the $^{13}C\{^1H\}$ NMR spectra. Like the dinuclear molecules **2**−**5**, both tetranuclear complexes **6** and **7** were obtained in relatively high yields of 87% and 71%, respectively. Additionally, two-dimensional NMR spectra of complex **7** confirmed its structure (see the Supporting Information, Figures S8−S11).

STRUCTURAL STUDIES

Single crystals of compounds **2**−**5** were obtained and provide detailed structural information on all four dinuclear species. X-

dx.doi.org/10.1021/ja400078c | J. Am. Chem. Soc. 2013, 135, 4051−4060

ray diffraction analysis of compound **2** (see Figure 1, Table 1 and Table S1 in the Supporting Information) showed a highly

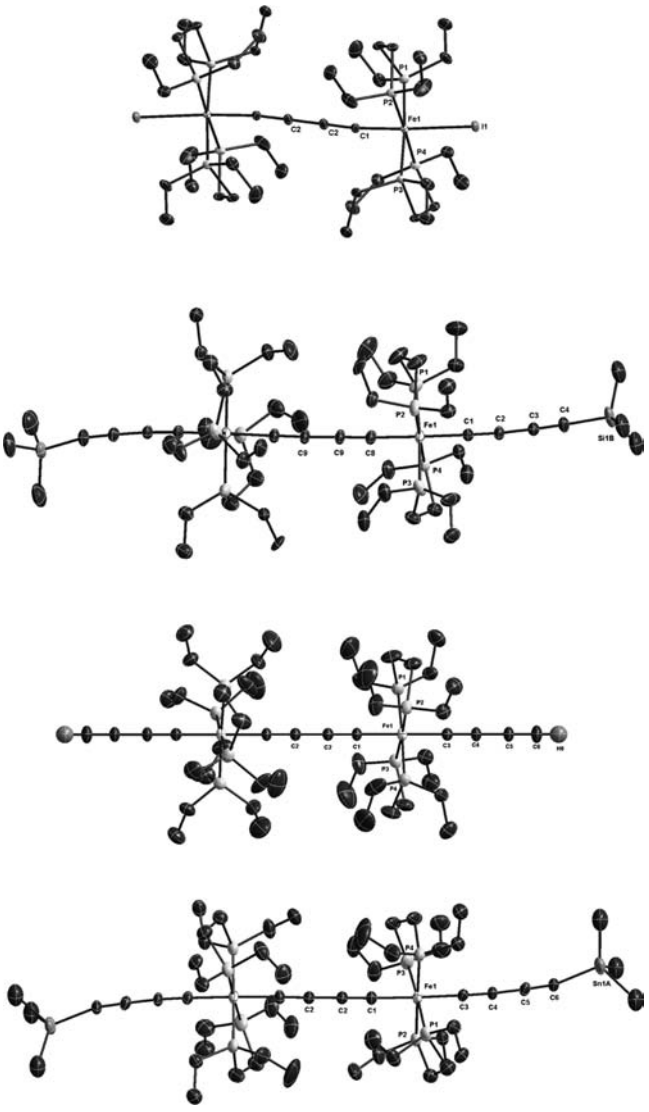

Figure 1. Molecular structures of **2** (top), **3** (upper middle), **4** (lower middle), and **5** (bottom). Ellipsoids are set at the 30% probability level. Solvent molecules and selected hydrogen atoms are omitted for clarity. See Table 1 for selected bond lengths, distances, and angles.

symmetric molecule possessing an inversion center located between C_B and $C_{B'}$ and revealed pseudo-octahedral geometries of the iron centers (see Figure 2 for the labeling of selected atoms).

The introduction of the bridging butadiynediyl ligand causes a contraction of the average Fe−P distance to 2.2469(6) Å compared to 2.309 Å in the mononuclear diiodo precursor,[42] which is consistent with an increase of σ-donation from the phosphine ligands to the iron centers. The length of the Fe−I bond remains at 2.7070(4) Å. The Fe−C_A bond is 1.889(2) Å, which agrees well with reported Fe−C(sp) bond lengths,[26,27,32] while the C_A—C_B (1.229(3) Å) and C_B—$C_{B'}$ (1.380(5) Å) bonds are in the range of C≡C and C—C bond lengths expected for a 1,3-butadiynediyl bridge.[50] The Fe−Fe distance is 7.6038(8) Å and is thus between the reported values of [CpFe(dppe)](μ-C_4)[50] and [(η^5-C_5Me_5)$(CO)_2Fe_2$](μ-C_4)[51] of 7.564 and 7.653 Å, respectively. The Fe−C_4−Fe axis in **2** shows a

Table 1. Selected Bond Lengths [Å], Nonbonding Distances [Å], and Angles [deg] of Compounds 2−5[a]

	2	3	4	5
Fe−C_A	1.889(2)	1.919(3)	1.916(6)	1.924(7)
C_A−C_B	1.229(3)	1.216(5)	1.221(9)	1.223(9)
C_B−$C_{B'}$	1.380(5)	1.389(7)	1.379(13)	1.381(12)
Fe−I	2.7070(4)			
Fe−C_C		1.907(3)	1.907(7)	1.908(6)
C_C−C_D		1.226(5)	1.220(9)	1.228(8)
C_D−C_E		1.371(5)	1.374(10)	1.371(9)
C_E−C_F		1.218(5)	1.181(10)	1.208(9)
Fe−P[b]	2.2469(6)	2.2292(12)	2.2250(9)	2.233(7)
Fe−Fe′	7.6038(8)	7.6525(8)	7.6515(12)	7.6590(9)
C_F−$C_{F'}$		19.048(5)	19.015(12)	19.035(9)
Fe−C_A−C_B	173.8(2)	178.3(3)	180	175.9(7)
C_A−$C_{B'}$−$C_{B'}$	179.3(4)	178.4(4)	180	178.5(7)
Fe−C_C−C_D		178.2(4)	180	177.8(7)
C_C−C_D−C_E		175.6(4)	180	176.3(7)
C_D−C_E−C_F		178.0(5)	180	177.9(9)

[a]Please refer to Figure 2 for the labeling. [b]Average bond length.

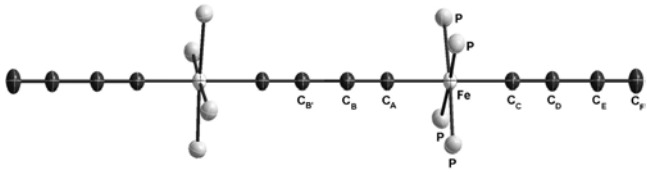

Figure 2. Labeling of selected atoms of the dinuclear complexes **3**−**5**. The atoms of complex **2** are labeled congruently.

slight deviation from linearity (173.8(2)° for Fe−C_A−C_B and 179.3(4)° for C_A−C_B−$C_{B'}$), which is commonly observed in L_mM−(C_4)−ML_m type complexes and mostly attributed to crystal packing effects.[52,53]

X-ray diffraction analyses of the three C_4R-disubstituted compounds (see Figure 1 for R = $SiMe_3$, H, and $SnMe_3$, respectively) showed structures with rigid-rod RC_4-{Fe}-C_4-{Fe}-C_4R backbones. Compared to the diiodo complex **2**, the Fe−Fe distance is clearly elongated (7.6525(8), 7.6515(12), and 7.6590(9) Å for R = $SiMe_3$, H, and $SnMe_3$, respectively) and assumes a value close to that of 7.653 Å found for [(η^5-C_5Me_5)$(CO)_2Fe_2$](μ-C_4).[51] This can be attributed to the even more pronounced butadiynediyl character of the bridge, marked by a slight contraction of the C_A−C_B triple bonds (see Figure 2 for the labeling of selected atoms), which is overcompensated by elongations of the Fe−C_A and C_B−$C_{B'}$ single bonds (see Table 1).

The symmetry of the structures is reduced compared to **2**, as the phosphine ligands are more staggered and, in case of **3** and **5**, the trimethylsilyl and trimethylstannyl groups capping the terminal butadiynyl ligands bend slightly out of plane. High symmetry is nevertheless retained for all three dinuclear C_4R substituted complexes. In particular, the C_4-Fe-C_4-Fe-C_4 backbone displays a rigid linearity with angles in the range of 175°−180° (see Table 1) and significantly less distortion than the dinuclear tungsten complexes described earlier.[18,26] The average Fe−P distance shows further contraction from the dinuclear diiodo **2** (2.2469(6) Å) to the C_4TMS capped compound **3** (2.2292(12) Å). This is consistent with a further decrease of the electron density of the metal centers due to the introduction of additional butadiynyl ligands and a resulting increase of the σ-donation of the phosphine ligands. Changes in the substitution of

dx.doi.org/10.1021/ja400078c | J. Am. Chem. Soc. 2013, 135, 4051−4060

the terminal C_F in the series from **2** to **5** have only a minor influence on the Fe−P distances (2.2250(9) and 2.233(7) Å on average for **4** and **5**, respectively). Further details on all structures are provided in the Supporting Information (Tables S1 and S2 and crystallographic information files).

CYCLIC VOLTAMMETRY

The cyclic voltammogram of **2** in THF/NBu_4PF_6 (see Figure S12 in the Supporting Information) exhibited two well-separated and reversible oxidation waves at $E_{1/2}$ = −905 and −362 mV vs Ag/AgCl ($Fc^{0/+}$ used as an external calibrant), marking the successive oxidation of the two metal centers. The K_c value of 1.9 × 10^9 (see Table 2) is in a very high range, indicating the large thermodynamic stabilization of the mixed valence species. No further waves were detected showing that the oxidation of the bridging ligand as described in the literature[33] lies outside the accessible solvent range or does not take place as the poorly π-donating iodo substituents in *trans* position to the bridge do not support this.

Table 2. Electrochemical Data of the Dinuclear Complexes[a]

compd	$E_{1/2}$(0/+1) [mV]	$E_{1/2}$(+1/+2) [mV]	ΔE [mV]	K_c	$E_{1/2}$(+2/+3) [mV]
2	−905	−362	543	1.9 × 10^9	
3	−863	−423	440	3.3 × 10^7	306
4	−880	−421	459	6.9 × 10^7	316
5	−893	−446	447	4.3 × 10^7	268

[a]Measurements at room temperature in THF/NBu_4PF_6 (0.1 M) with an Au working electrode, a Pt counter electrode, and a nonaqueous reference electrode (Ag/AgCl). Calibrated against $Fc^{0/+}$ as an external calibrant.

Three well-separated and reversible oxidation waves (see Figure 3, Table 2 and section Spectroelectrochemical Studies) were observed in the cyclic voltammogram of **3**, marking the successive oxidation of the two metal centers and subsequently the oxidation of the bridging ligand. While the K_c value for the radical cation decreased by 2 orders of magnitude when compared to **2**, it is still very high, indicating the high stability of the mixed valence Fe(II)/Fe(III) form.

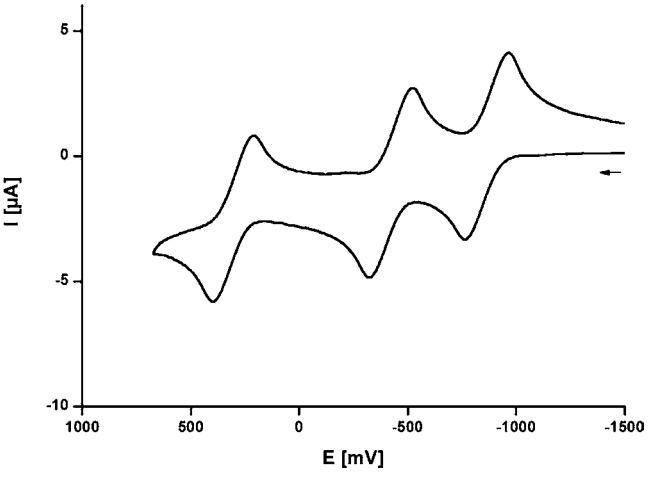

Figure 3. Cyclic voltammogram for **3** in THF/NBu_4PF_6 (0.1 M) at room temperature; Au electrode; *E* vs $Fc^{0/+}$ (external).

The electrochemical properties of compounds **4** and **5** were found to be similar to complex **3**. Both showed three reversible oxidation waves occurring at potentials similar to **3** (see Table 2 and Figures S13 and S14 in the Supporting Information) as well as K_c values in a similar range. This is in line with our expectations due to the high structural similarity of complexes **3**, **4**, and **5**.

The cyclic voltammetric study of **6** in CH_2Cl_2/NBu_4PF_6 (vs Ag/AgCl, $Fc^{0/+}$ used as an external calibrant) exhibited four individually resolved, reversible oxidation waves (see Figure 4 and Table 3), marking the successive oxidation of all four metal centers. The oxidations were observed at very negative potentials with E° = −1434, −1099, −650, and −435 mV. Similar to **6**, the second tetranuclear compound **7** underwent four successive oxidations in the cyclic voltammogram (see Figure S15 in the Supporting Information, Table 3, and section Spectroelectrochemical Studies), attributable to the stepwise oxidation of the four metal centers.

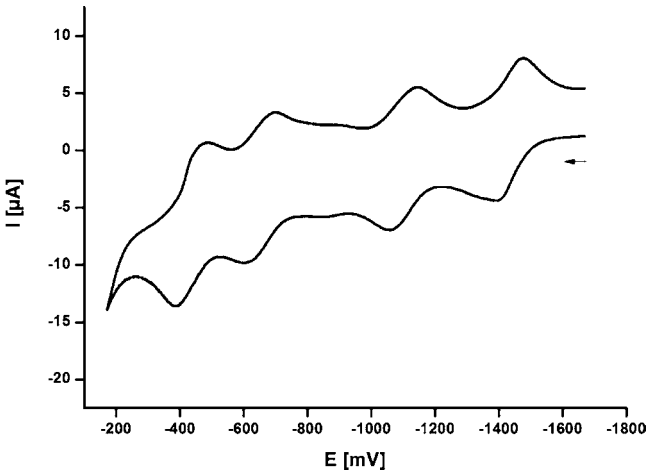

Figure 4. Cyclic voltammogram for **6** in CH_2Cl_2/NBu_4PF_6 (0.1M) at room temperature; Au electrode; *E* vs $Fc^{0/+}$ (external).

Neither complex **6** nor complex **7** exhibited further reversible oxidation waves within the potential window of the given electrolyte that could be attributed to redox processes of the organic units. It has to be noted that the successive oxidations of the metal centers occur at very negative potentials, while the oxidation of the carbon-rich bridging ligand of **3**, **4**, and **5** was observed at a much more positive potential. The separations of individual half-wave potentials for both tetranuclear compounds are not as large as for the dinuclear complexes, but still substantial and well sufficient to allow a spectroelectrochemical probing of individual oxidation states.

SPECTROELECTROCHEMICAL STUDIES

Complexes **2**, **3**, and **7** were selected for spectroelectrochemical experiments that aimed at probing the electron delocalization along the metal−organic π-conjugated chain through the changes in the ν(C≡C) band pattern and intensities upon stepwise oxidation. Complex **2** features only the internal butadiynediyl ligand and can thus be used to identify the vibrational bands of the $[\{Fe\}—C{\equiv}C—C{\equiv}C—\{Fe\}]^{n+}$ core without interference of the additional C_4R ligands of complexes **3** and **7**.

Spectroelectrochemical studies on complex **2** suffered from its low solubility in the THF/NBu_4PF_6 supporting electrolyte and its inherent instability in chlorinated solvents, such that the signal-to-noise ratio of the spectra is rather poor (see Figures S16 and S17 of the Supporting Information).

dx.doi.org/10.1021/ja400078c | J. Am. Chem. Soc. 2013, 135, 4051−4060

Table 3. Electrochemical Data for the Tetranuclear Complexes[a]

compd	$E_{1/2}(0/+1)$ [mV]	$E_{1/2}(+1/+2)$ [mV]	$\Delta E_{(1,2)}$ [mV]	$E_{1/2}(+2/+3)$ [mV]	$\Delta E_{(2,3)}$ [mV]	$E_{1/2}(+3/+4)$ [mV]	$\Delta E_{(3,4)}$ [mV]
6[b]	−1434	−1099	335	−650	449	−435	215
7[c]	−1204	−873	331	−553	320	−421	135

[a]Measurements performed with an Au working electrode and a Pt counter electrode, and a nonaqueous reference electrode (Ag/AgCl). Calibrated against $Fc^{0/+}$ as an external calibrant. [b]In THF/Bu_4NPF_6 (0.1M) at room temperature. [c]In CH_2Cl_2/Bu_4NPF_6 (0.1M) at room temperature.

Table 4. IR ν(C≡C) data (in cm^{-1}) for the Complexes in Their Various Oxidation States

	$n = 0$	$n = 1$	$n = 2$
$\mathbf{2}^{n+}$ [a]	1951	1972, 1880	not observed
$\mathbf{3}^{n+}$ [b]	2157, 2100(sh), 2068, 1967(sh), 1951	2153, 2106, 2080(sh), 1990, 1964, 1955(sh), 1878	2157, 2104, 2080(sh), 2030, 1958(sh), 1937, 1878
$\mathbf{7}^{n+}$	2155, 2073, 2043(sh), 1965(sh), 1947, 1924, 1885	2152, 2096(sh), 2085, 2035, 1947(sh), 1930, 1882	2152, 2102, 2075(sh), 2037, 1925, 1882(sh), 1799

[a]In THF/NBu_4PF_6 (0.2 M) as the supporting electrolyte. [b]In 1,2-$C_2H_4Cl_2$/$NBu_4BAr^F{}_4$ ($BAr^F{}_4$ = $B\{C_6H_3(CF_3)_2\text{-}3,5\}_4^-$) (0.1 M) as the supporting electrolyte.

In contrast to Lapinte's butadiynediyl-bridged diiron complexes with Cp*Fe(LL) half-sandwich type end groups, neutral **2** displays just one C≡C IR stretch in its IR spectrum at almost the same energy as the higher energy band of the Cp*Fe(dppe) analogue.[54] We note, however, that similar C_4-bridged diruthenium, diosmium, or dirhenium complexes usually display just one C≡C band in their IR spectra[17,55−59] while other rigid-rod like dimetal complexes with the higher local D_{2h} symmetry of **2** may display no IR-active C≡C vibration at all.[60,61]

Upon oxidation, the single ν(C≡C) band of **2** at 1951 cm^{-1} evolves into a two-band pattern with peaks at 1972 and 1880 cm^{-1} (see Table 4). One might argue that this observation points to the loss of a centrosymmetric structure upon oxidation and hence to a valence-localized structure with discernible Fe(II) and Fe(III) sites on the IR time scale. The observation of a pattern of two ν(C≡C) bands for mixed-valent butadiynediyl-bridged dimetal complexes of Class III with intrinsic charge delocalization is, however, not without precedence, in particular in iron chemistry.[54,62] We also note the growth of an intense, broad near-infrared (NIR) band of electronic origin peaking at 6400 cm^{-1} (1560 nm) (see Figure S16). With reference to the mixed-valent radical cations of the aforementioned half-sandwich diiron complexes this band is assigned as the Fe(II)→Fe(III) intervalence charge transfer (IVCT) absorption. This IVCT band is truncated at the low energy side with half widths of 1270 cm^{-1} at higher energy of the maximum and 1020 cm^{-1} at the lower energy side. Both half-widths are substantially lower than the value expected of a Class II system, $\Delta\nu_{1/2} = (2310\nu_{max})^{1/2}$ = 3750 cm^{-1}, derived from Hush's theory.[63,64] Brunschwig, Creutz, and Sutin have introduced the Γ value with $\Gamma = 1 - \nu_{1/2,obsd}/\nu_{1/2,calc}$ as a measure of ground state delocalization.[65] The value of 0.66 obtained for the half-width at the higher energy realm clearly exceeds the value of 0.50 delimiting the Class II−III transition and hence points to extensive charge delocalization in this mixed-valence species.

Further oxidation at a potential positive of the +/2+ couple results in a further increase of the intensity of the ν(C≡C) IR band at the lower energy and a slight shift to 1883 cm^{-1} as well as a partial bleaching of the low-energy electronic band. Longer electrolysis times and a further increase of the applied potential led to an intensity loss of all vibrations that precludes a firm assignment of the spectroscopic properties of that species. Preliminary studies of chemically oxidized $\mathbf{2}^+$ and $\mathbf{2}^{2+}$ showed that they are reasonably stable compounds. It was however observed that $\mathbf{2}^{2+}$ is completely insoluble in THF, which could be a reason for the observed behavior.

Replacement of the terminal iodo ligands by trimethylsilylbutadiynyl ones leads to extensive vibrational coupling along the unsaturated −C_4−{Fe}−C_4−{Fe}−C_4− backbone as can be inferred from the large number of alkynyl stretching vibrations for neutral **3** that spread over the 2157 to 1951 cm^{-1} range. Upon oxidation to its radical cation in the 1,2-$C_2H_4Cl_2$/$NBu_4BAr^F{}_4$ ($BAr^F{}_4^-$ = $B\{C_6H_3(CF_3)_2\text{-}3,5\}_4^-$) electrolyte, the number of IR active vibrations further increases (see Table 4 and Figure 5).

By inference from $\mathbf{2}^{0/+}$, the stretches at 1951 cm^{-1} of **3** and at 1964 and 1878 cm^{-1} of $\mathbf{3}^+$ can be assigned to vibrational modes of the central butadiynediyl ligand. The ν(C≡C) band positions of that entity thus seem to be only little affected by substitution at the *trans*-disposed terminal ligands. Oxidation of one of the core

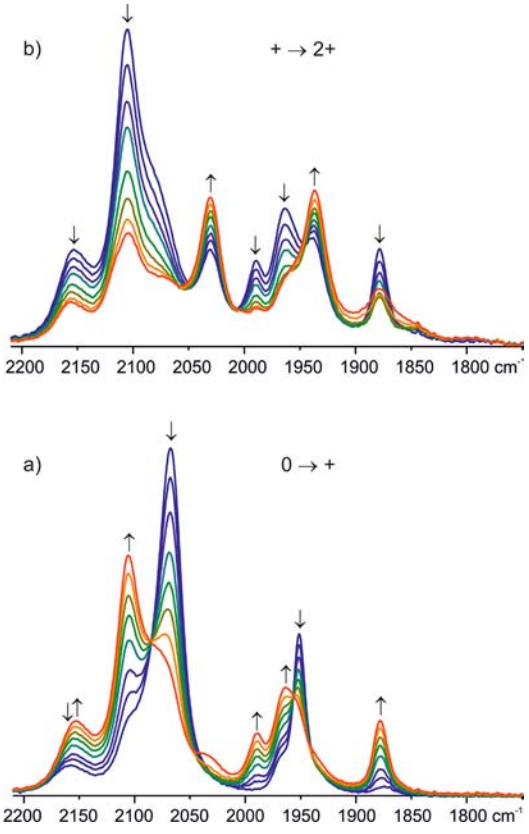

Figure 5. IR spectroscopic changes during (a) the first and (b) the second oxidation of complex **3** in an OTTLE cell (1,2-$C_2H_4Cl_2$/$NBu_4BAr^F{}_4$ 0.2 M at room temperature).

dx.doi.org/10.1021/ja400078c | J. Am. Chem. Soc. 2013, 135, 4051−4060

Fe atoms likewise seems to have rather little influence on the energies of the ν(C≡C) modes of the terminal ligands while there are changes in terms of relative band intensities. This is most clearly seen for the prominent band of the butadiynyl ligands, where the pattern of a high-energy shoulder at 2100 cm^{-1} and a main peak at 2068 cm^{-1} just inverses upon oxidation with only slight shifts to result in a strong peak at 2106 cm^{-1} and a shoulder at 2080 cm^{1}. We concede, however, that such reasoning might be too simplistic when considering the strong coupling between the individual vibrators along the unsaturated TMS−C_4−{Fe}−C_4−{Fe}−C_4−TMS chain.

Further oxidation to $\mathbf{3}^{2+}$ bleaches the bands at 1990 and 1964 cm^{-1}, while the remaining ones experience only small shifts but larger changes in intensity. Again, this second oxidation process could not be pursued to full conversion before the onset of irreversible spectroscopic changes which might again be due to insufficient solubility of oxidized $\mathbf{3}^{2+}$. This unfortunately precludes us from assessing the spectroscopic changes associated with the third oxidation. Similar experiments in the THF/NBu_4PF_6 electrolyte produced almost identical results for the **3**/$\mathbf{3}^{+}$ pair of compounds as in the 1,2-$C_2H_4Cl_2$/$NBu_4BAr^F{}_4$ electrolyte (see Figure S18 of the Supporting Information) but failed to produce reliable results for even $\mathbf{3}^{2+}$. Of note is the observation of a low-energy electronic band at 6040 cm^{-1} (1655 nm) that grows in during the first oxidation of **3** and bleaches during the second one. This feature is also seen as a strong band at 6145 cm^{-1} (1627 nm) in UV/vis/NIR spectroelectrochemistry (see Figure 6) with additional shoulders at 7300 and 8064 cm^{-1} (1370 and 1240 nm). The energy of this band falls close to the equivalent absorption of $\mathbf{2}^{+}$ at 1560 nm (6400 cm^{-1}) and is again assigned as an Fe(II)→Fe(III) IVCT. As for $\mathbf{2}^{+}$ this band is truncated at the low energy side with half widths of 1510 and 1290 cm^{-1}, respectively, for the high- and low-energy realms of the peak. The ratio θ between the observed half-width and the calculated one of a Class II system is 0.40, which in turn yields a Γ value of 0.60. This value is again larger than the one of 0.50 marking the Class II−III transition. This argues for strong electronic coupling between the C_4-bridged {Fe} sites in $\mathbf{3}^{+}$. Other changes in the UV/vis part of the spectrum include the shift of the original UV band from 341 to 322 nm and the growth of weaker shoulders at 394 and 420 nm as well as an additional small peak at 720 nm. On oxidation to the $\mathbf{3}^{2+}$ dication the original NIR absorption is bleached with the concomitant growth of a new structured band of like absorptivity at 1015 nm and a shoulder to the blue at 970 nm. For this band we propose $\pi\rightarrow\pi^*$-parentage, most probably with strong ligand-to-metal charge-transfer contributions. Like bands, albeit usually at lower energies, are routinely observed for Fe(III) alkynyl complexes including other butadiynediyl-bridged diiron complexes with half-sandwich-type {Fe} sites.[54,62,66]

Further elongation of the rigid-rod metal organic π-system to the tris(butadiynediyl)-bridged tetrairon complex **7** results in a further increase of the number of IR active modes in the 1965 to 1885 cm^{-1} range along with a red shift of the prominent C≡C absorption from 1951 to 1924 cm^{-1} (see Figure 7). This is probably the result of further vibrational coupling between the two central butadiynediyl ligands. Similar to **3**, oxidation of **7** to its radical cation caused a blue shift of the main peak of the bands assigned to the terminal butadiynyl ligands from 2073 to 2085 cm^{-1} and an intensity increase of the vibrations at 1947 and 1924 cm^{-1}, but hardly any change in their positions. The second oxidation likewise causes changes in band intensities rather than band positions with the exception of the growth of an intense band at 1799 cm^{-1}. This feature resembles the low-energy band formed upon the first oxidation of complexes **2** and **3**, yet with a

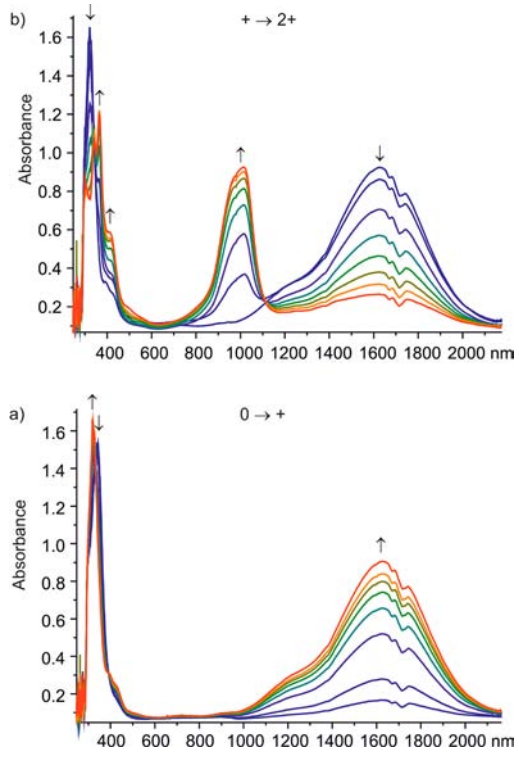

Figure 6. UV/vis/NIR spectroscopic changes during (a) the first and (b) the second oxidation of complex **3** in an OTTLE cell (1,2-$C_2H_4Cl_2$/$NBu_4BAr^F{}_4$ 0.2 M at room temperature).

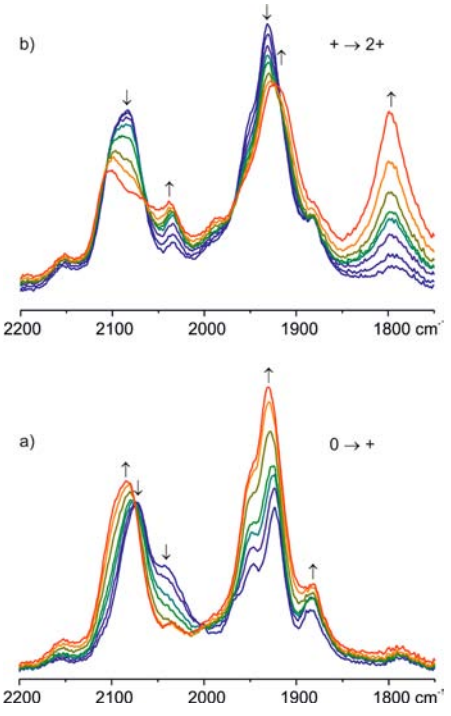

Figure 7. IR spectroscopic changes during (a) the first and (b) the second oxidation of complex **7** in the mid-IR in an OTTLE cell (1,2-$C_2H_4Cl_2$/$NBu_4BAr^F{}_4$ 0.2 M at room temperature).

dx.doi.org/10.1021/ja400078c | J. Am. Chem. Soc. 2013, 135, 4051−4060

substantial red shift of ca. 80 cm^{-1}. Just like 2^+ and 3^+, radical cation 7^+ displays a broad, strong NIR absorption at ca. 5500 cm^{-1} (1820 nm, see Figure 8). This band has a rather symmetrical shape.

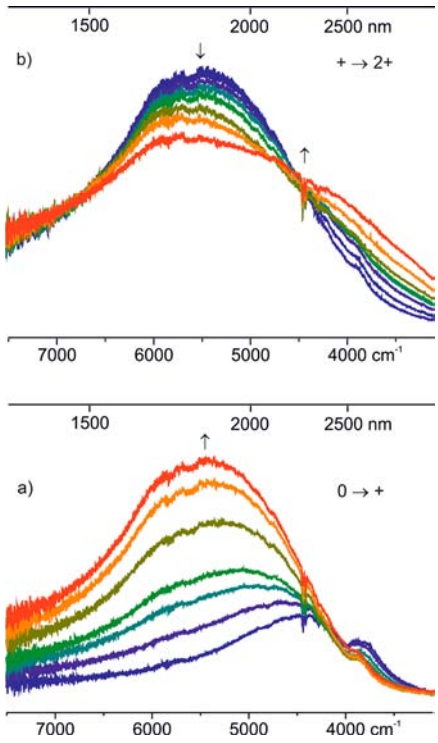

Figure 8. IR spectroscopic changes during (a) the first and (b) the second oxidation of complex **7** in the NIR in an OTTLE cell (1,2-$C_2H_4Cl_2$/$NBu_4BAr^F{}_4$ 0.2 M at room temperature).

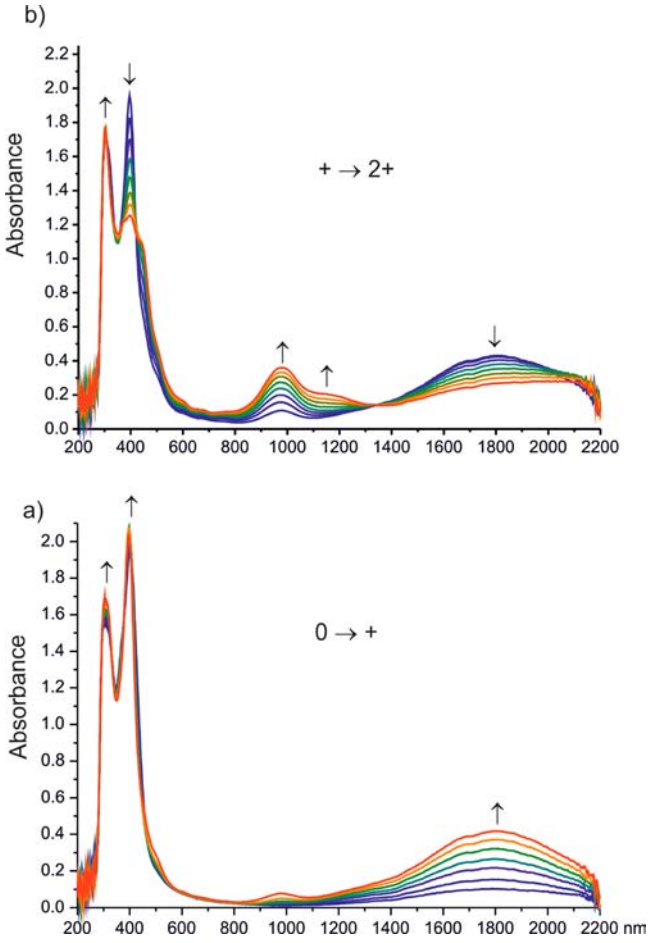

Figure 9. UV/vis/NIR spectroscopic changes during (a) the first and (b) the second oxidation of complex **7** in an OTTLE cell (1,2-$C_2H_4Cl_2$/$NBu_4BAr^F{}_4$ 0.2 M at room temperature).

As shown in Figure 9, this band is also observed in UV/vis/NIR spectroelectrochemical experiments and displays a half width of ca. 1750 cm^{-1}, which is again appreciably smaller than the value of 3565 cm^{-1} derived from the Hush formula for a Class II system but appreciably larger as for 2^+ and 3^+. The calculated Γ value of 0.51 places 7^+ still in the regime of strongly delocalized systems, yet at the Class II/III borderline. Spectral deconvolution of the NIR part of the electronic spectrum reveals the presence of a second, broader NIR band peaking at 6920 cm^{-1} (1445 nm) with a half-width of 3010 cm^{-1} (see Figure S19 of the Supporting Information). The calculated Γ value of 0.25 is typical of an IVCT transition within a mixed-valent system of Class II parentage. Other spectroscopic changes along the $7/7^+/7^{2+}$ redox system are similar to complex **3**, i.e. some slight shift and intensity increase of the prominent UV and vis bands and the growth of a shoulder at 495 nm during the first oxidation and the development of a structured NIR band with resolved peaks at 977 and 1177 nm upon the second oxidation. Of note is a moderate red shift of these bands when compared to 3^{2+}, obviously as a consequence of the further extension of the π-conjugated pathway. At variance with 3^{2+}, doubly oxidized 7^{2+} still retains a rather strong NIR band at 5065 cm^{-1} (1970 nm), that is at a just slightly higher energy as the equivalent IR band of 7^+.

Deconvolution of the NIR part of the electronic spectrum of 7^{2+} (see Figure S19 of the Supporting Information) provides an excellent fit to the experimental spectra and indicates that the low-energy NIR absorption originates from a single absorption with a half-width of 2690 cm^{-1}, corresponding to a Γ value of 0.21.

This finding possibly provides a clue to the sequence of oxidations within the bis(butadiynediyl)-bridged tetrairon core. One can reasonably assume that a $Fe(depe)_2$-substituted butadiynyl moiety is more electron rich than a TMS-substituted one. Hence, one of the inner two {Fe} sites with two attached $-C_4-${Fe}$-C_4-$TMS "ligands" is a more likely candidate for the primary oxidation site. For the TMS$-C_4-${Fe}$-C_4-${Fe}$^+-C_4-${Fe}$-C_4-${Fe}$-C_4-$TMS system thus formed one might expect two IVCT transitions from electronically different neighboring {Fe} sites. This assumes that IVCT from the next-to-nearest neighbors, i.e. from the remote TMS$-C_4-${Fe}$-$ moiety, is not observed. The second oxidation could then occur at either the remaining central or one of the remote terminal {$Fe(depe)_2$bis(butadiynyl)} sites (see Figure 10). Oxidation of the remaining inner moiety (I in Figure 10) would lead to a system where only one type of IVCT transition, that is from each of the outer to the neighboring inner site, is observed.

In that case one would also expect that the remaining IVCT band is the one displaying the weaker electronic coupling. Both these expectations match with our experimental observations. We also note that the appreciably smaller Γ value for the IVCT transition between the inner sites when compared to 2^+ and 3^+ correlates with the likewise smaller $\Delta E_{1/2}$ and K_c values for radical cation 7^+ when compared to 2^+ and 3^+.

dx.doi.org/10.1021/ja400078c | J. Am. Chem. Soc. 2013, 135, 4051−4060

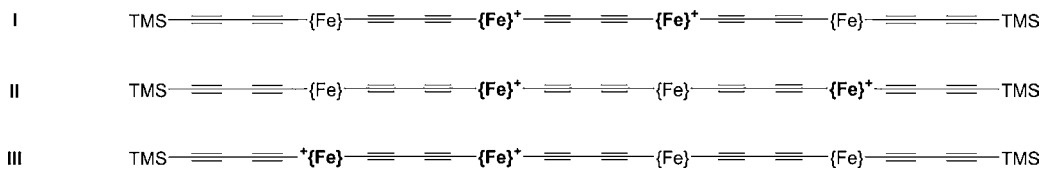

Figure 10. Possible electronic structures of the dication 7^{2+}.

Considering that the only difference between 2^+, 3^+, and 7^+ is the identity of the peripheral ligand (−I, $-C_4-$TMS or $-C_4-${Fe}$-C_4-$TMS) and that spatial distances between the {Fe}-based redox sites in these complexes are virtually identical, the decrease of the $\Delta E_{1/2}$ and K_c values is very likely of true electronic origin as opposed to electrostatic effects, changes in the inductive effects or magnetic exchange term.[67−69] The other possibility is that the second oxidation involves one of the terminal {Fe} sites. Electrostatic repulsion between like unipositively charged redox centers one would make an oxidation of the remote moiety more feasible than that of the one neighboring the already oxidized site, thus rendering a dication with two chemically different oxidized $\{Fe\}^+$ sites (II in Figure 10). In such a case one would expect to see three IVCT transitions, one arising from charge transfer from the reduced inner to the oxidized inner, one from the reduced inner to the oxidized outer, and one from the reduced outer to the oxidized inner {Fe} moiety. The third, least likely scenario of the second oxidation involues the outer {Fe} moiety neighboring the already oxidized inner one (III in Figure 10). Here, one would also expect to see a single IVCT band, but this time the one with the stronger coupling. This is, of course, under the assumption that our assignments of the IVCT transitions of 7^+ are correct. Unfortunately, all attempts to assess the higher oxidized forms of **7** proved to be in vain.

CONCLUSION

In summary, we have demonstrated that a stepwise construction of homometallic tetranuclear species starting from a diiron *trans* diiodo complex could be achieved proving that long and well-defined rigid-rod organometallic molecules with tunable redox properties are accessible via a controlled and iterative synthesis. To the best of our knowledge this is the first report of a tetranuclear homometallic species that still has intrinsically open terminal binding sites. Also, the investigated compounds display IVCT between the metal centers as well as a high stabilization of its oxidized forms. Complexes **2**, **5**, and **6** are excellent starting materials for even longer scaffolds with even or odd numbers of metal centers along a fully conjugated rigid-rod like metal−organic backbone that could pave the way to materials with unique electronic properties. We also note that the elucidation of the individual transfer sites in such systems, the interpretation of vibrational patterns, and the nature of the electronic transitions becomes a more and more demanding task as the number of redox sites increases.

ASSOCIATED CONTENT

Supporting Information

Experimental details including more detail on NMR spectroscopy (Figures S1−S11), cyclic voltammetry (Figures S12−S15), and spectroeletrochemical studies (Figures S16−S19) as well as summaries of the X-ray diffraction studies (Table S1 and S2). This material is available free of charge via the Internet at http://pubs.acs.org.

AUTHOR INFORMATION

Corresponding Author

hberke@aci.uzh.ch

Notes

The authors declare no competing financial interest.

ACKNOWLEDGMENTS

Funding from the National Research Programme "Smart Materials" (NRP 62, grant no. 406240-126142) of the Swiss National Science Foundation (SNSF) and the University of Zürich is gratefully acknowledged.

REFERENCES

(1) Metzger, R. M. *J. Mater. Chem.* **2008**, *18*, 4364.
(2) Vuillaume, D. *C. R. Phys.* **2008**, *9*, 78.
(3) Carroll, R. L.; Gorman, C. B. *Angew. Chem., Int. Ed.* **2002**, *41*, 4378.
(4) Luo, L. A.; Choi, S. H.; Frisbie, C. D. *Chem. Mater.* **2011**, *23*, 631.
(5) Brédas, J.-L.; Beljonne, D.; Coropceanu, V.; Cornil, J. *Chem. Rev.* **2004**, *104*, 4971.
(6) Choi, S. H.; Kim, B.; Frisbie, C. D. *Science* **2008**, *320*, 1482.
(7) Lu, Q.; Liu, K.; Zhang, H. M.; Du, Z. B.; Wang, X. H.; Wang, F. S. *ACS Nano* **2009**, *3*, 3861.
(8) Tuccitto, N.; Ferri, V.; Cavazzini, M.; Quici, S.; Zhavnerko, G.; Licciardello, A.; Rampi, M. A. *Nat. Mater.* **2009**, *8*, 359.
(9) Aguirre-Etcheverry, P.; O'Hare, D. *Chem. Rev.* **2010**, *110*, 4839.
(10) Ceccon, A.; Santi, S.; Orian, L.; Bisello, A. *Coord. Chem. Rev.* **2004**, *248*, 683.
(11) Low, P. J. *Coord. Chem. Rev.* **2012**, DOI: 10.1016/j.ccr.2012.08.008.
(12) Bruce, M. I.; Le Guennic, B.; Scoleri, N.; Zaitseva, N. N.; Halet, J.-F. *Organometallics* **2012**, *31*, 4701.
(13) Yu, M. P. Y.; Yam, V. W.-W.; Cheung, K.-K.; Mayr, A. *J. Organomet. Chem.* **2006**, *691*, 4514.
(14) Gauthier, N.; Argouarch, G.; Paul, F.; Humphrey, M. G.; Toupet, L.; Ababou-Girard, S.; Sabbah, H.; Hapiot, P.; Fabre, B. *Adv. Mater.* **2008**, *20*, 1952.
(15) Wuttke, E.; Pevny, F.; Hervault, Y. M.; Norel, L.; Drescher, M.; Winter, R. F.; Rigaut, S. *Inorg. Chem.* **2012**, *51*, 1902.
(16) Pevny, F.; Di Piazza, E.; Norel, L.; Drescher, M.; Winter, R. F.; Rigaut, S. *Organometallics* **2010**, *29*, 5912.
(17) Bruce, M. I.; Low, P. J.; Costuas, K.; Halet, J.-F.; Best, S. P.; Heath, G. A. *J. Am. Chem. Soc.* **2000**, *122*, 1949.
(18) Semenov, S. N.; Blacque, O.; Fox, T.; Venkatesan, K.; Berke, H. *J. Am. Chem. Soc.* **2010**, *132*, 3115.
(19) Venkatesan, K.; Blacque, O.; Berke, H. *Dalton Trans.* **2007**, 1091.
(20) Egler-Lucas, C.; Blacque, O.; Venkatesan, K.; López-Hernández, A.; Berke, H. *Eur. J. Inorg. Chem.* **2012**, *2012*, 1536.
(21) Zheng, Q.; Hampel, F.; Gladysz, J. A. *Organometallics* **2004**, *23*, 5896.
(22) Olivier, C.; Kim, B.; Touchard, D.; Rigaut, S. *Organometallics* **2008**, *27*, 509.
(23) Benameur, A.; Brignou, P.; Di Piazza, E.; Hervault, Y. M.; Norel, L.; Rigaut, S. *New J. Chem.* **2011**, *35*, 2105.
(24) Luo, L.; Benameur, A.; Brignou, P.; Choi, S. H.; Rigaut, S.; Frisbie, C. D. *J. Phys. Chem. C* **2011**, *115*, 19955.
(25) Field, L. D.; Turnbull, A. J.; Turner, P. *J. Am. Chem. Soc.* **2002**, *124*, 3692.

(26) Semenov, S. N.; Taghipourian, S. F.; Blacque, O.; Fox, T.; Venkatesan, K.; Berke, H. *J. Am. Chem. Soc.* **2010**, *132*, 7584.
(27) De Montigny, F.; Argouarch, G.; Costuas, K.; Halet, J. F.; Roisnel, T.; Toupet, L.; Lapinte, C. *Organometallics* **2005**, *24*, 4558.
(28) Frohnapfel, D. S.; Woodworth, B. E.; Thorp, H. H.; Templeton, J. L. *J. Phys. Chem. A* **1998**, *102*, 5665.
(29) Costuas, K.; Rigaut, S. *Dalton Trans.* **2011**, *40*, 5643.
(30) Paul, F.; Lapinte, C. *Coord. Chem. Rev.* **1998**, *178*−*180* (Part 1), 431.
(31) Halet, J.-F.; Lapinte, C. *Coord. Chem. Rev.* **2012**, DOI: 10.1016/j.ccr.2012.09.007.
(32) Bruce, M. I.; Costuas, K.; Davin, T.; Ellis, B. G.; Halet, J. F.; Lapinte, C.; Low, P. J.; Smith, M. E.; Skelton, B. W.; Toupet, L.; White, A. H. *Organometallics* **2005**, *24*, 3864.
(33) Guillemot, M.; Toupet, L.; Lapinte, C. *Organometallics* **1998**, *17*, 1928.
(34) Iyer, R. S.; Selegue, J. P. *J. Am. Chem. Soc.* **1987**, *109*, 910.
(35) Le Narvor, N.; Toupet, L.; Lapinte, C. *J. Am. Chem. Soc.* **1995**, *117*, 7129.
(36) Hoffert, W. A.; Rappe, A. K.; Shores, M. P. *Chem. Commun.* **2010**, *46*, 4710.
(37) Colbert, M. C. B.; Lewis, J.; Long, N. J.; Raithby, P. R.; Younus, M.; White, A. J. P.; Williams, D. J.; Payne, N. N.; Yellowlees, L.; Beljonne, D.; Chawdhury, N.; Friend, R. H. *Organometallics* **1998**, *17*, 3034.
(38) Field, L. D.; George, A. V.; Laschi, F.; Malouf, E. Y.; Zanello, P. *J. Organomet. Chem.* **1992**, *435*, 347.
(39) Baker, M. V.; Field, L. D.; Hambley, T. W. *Inorg. Chem.* **1988**, *27*, 2872.
(40) Allen, O. R.; Dalgarno, S. J.; Field, L. D.; Jensen, P.; Tumbull, A. J.; Willis, A. C. *Organometallics* **2008**, *27*, 2092.
(41) Field, L. D.; Li, H. L.; Dalgarno, S. J.; Turner, P. *Chem. Commun.* **2008**, 1680.
(42) Barclay, J. E.; Hills, A.; Hughes, D. L.; Leigh, G. J. *J. Chem. Soc., Dalton Trans.* **1988**, 2871.
(43) Taghipourian, S. F.; Berke, H. Unpublished Results.
(44) Bancroft, G. M.; Mays, M. J.; Prater, B. E. *J. Chem. Soc. A* **1970**, 956.
(45) Semenov, S. N.; Blacque, O.; Fox, T.; Venkatesan, K.; Berke, H. *Organometallics* **2010**, *29*, 6321.
(46) Lewis, J.; Khan, M. S.; Kakkar, A. K.; Raithby, P. R.; Fuhrmann, K.; Friend, R. H. *J. Organomet. Chem.* **1992**, *433*, 135.
(47) Adams, R. D.; Davison, A.; Selegue, J. P. *J. Am. Chem. Soc.* **1979**, *101*, 7232.
(48) Holmes, A. B.; Jones, G. E. *Tetrahedron Lett.* **1980**, *21*, 3111.
(49) Jones, K.; Lappert, M. F. *J. Chem. Soc.* **1965**, 1944.
(50) Jiao, H. J.; Costuas, K.; Gladysz, J. A.; Halet, J. F.; Guillemot, M.; Toupet, L.; Paul, F.; Lapinte, C. *J. Am. Chem. Soc.* **2003**, *125*, 9511.
(51) Akita, M.; Chung, M. C.; Sakurai, A.; Sugimoto, S.; Terada, M.; Tanaka, M.; Morooka, Y. *Organometallics* **1997**, *16*, 4882.
(52) Dembinski, R.; Lis, T.; Szafert, S.; Mayne, C. L.; Bartik, T.; Gladysz, J. A. *J. Organomet. Chem.* **1999**, *578*, 229.
(53) Szafert, S.; Gladysz, J. A. *Chem. Rev.* **2003**, *103*, 4175.
(54) Le Narvor, N.; Toupet, L.; Lapinte, C. *J. Am. Chem. Soc.* **1995**, *117*, 7129.
(55) Bruce, M. I.; Ellis, B. G.; Low, P. J.; Skelton, B. W.; White, A. H. *Organometallics* **2003**, *22*, 3184.
(56) Bruce, M. I.; Costuas, K.; Davin, T.; Halet, J.-F.; Kramarczuk, K. A.; Low, P. J.; Nicholson, B. K.; Perkins, G. J.; Roberts, R. L.; Skelton, B. W.; Smith, M. E.; White, A. H. *Dalton Trans.* **2007**, 5387.
(57) Meyer, W. E.; Amoroso, A. J.; Horn, C. R.; Jaeger, M.; Gladysz, J. A. *Organometallics* **2001**, *20*, 1115.
(58) Brady, M.; Weng, W.; Zhou, Y.; Seyler, J. W.; Amoroso, A. J.; Arif, A. M.; Böhme, M.; Frenking, G.; Gladysz, J. A. *J. Am. Chem. Soc.* **1997**, *119*, 775.
(59) Roberts, R. L.; Puschmann, H.; Howard, J. A. K.; Yamamoto, J. H.; Carty, A. J.; Low, P. J. *Dalton Trans.* **2003**, 1099.
(60) Fernández, F. J.; Blacque, O.; Alfonso, M.; Berke, H. *Chem. Commun.* **2001**, 1266.
(61) Mohr, W.; Stahl, J.; Hampel, F.; Gladysz, J. A. *Chem.—Eur. J.* **2003**, *9*, 3324.
(62) Le Narvor, N.; Lapinte, C. *J. Chem. Soc., Chem. Commun.* **1993**, 357.
(63) Hush, N. S. *Prog. Inorg. Chem.* **1967**, *8*, 391.
(64) Hush, N. S. *Coord. Chem. Rev.* **1985**, *64*, 135.
(65) Brunschwig, B.; Creutz, C.; Sutin, N. *Chem. Soc. Rev.* **2002**, *31*, 168.
(66) Paul, F.; Toupet, L.; Thépot, J.-Y.; Costuas, K.; Halet, J.-F.; Lapinte, C. *Organometallics* **2005**, *24*, 5464.
(67) Sutton, J. E.; Sutton, P. M.; Taube, H. *Inorg. Chem.* **1979**, *18*, 1017.
(68) Evans, C. E. B.; Naklicki, M. L.; Rezvani, A. R.; White, C. A.; Kondratiev, V. V.; Crutchley, R. J. *J. Am. Chem. Soc.* **1998**, *120*, 13096.
(69) Lin, Y.-C.; Chen, W.-T.; Tai, J.; Su, D.; Huang, S.-Y.; Lin, I.; Lin, J.-L.; Lee, M. M.; Chiou, M. F.; Liu, Y.-H.; Kwan, K.-S.; Chen, Y.-J.; Chen, H.-Y. *Inorg. Chem.* **2009**, *48*, 1857.